Measurements of the ground-state ionization energy and wavelengths for the $1s^2\,{}^1S_0-1snp\,{}^1P_1$ $(n=6-12)$ lines of Al XII

A. L. Osterheld
Lawrence Livermore National Laboratory, Livermore, California 94551

A. I. Magunov, V. M. Dyakin, A. Ya. Faenov, T. A. Pikuz, and I. Yu. Skobelev
Multicharged Ions Spectra Data Center, VNIIFTRI, Mendeleevo, 141570 Moscow Region, Russia

T. Pisarczyk, P. Parys, J. Wolowski, and J. Makowski
Institute of Plasma Physics and Laser Microfusion, Warsaw, Poland

S. A. Pikuz, V. M. Romanova, and T. A. Shelkovenko
P. N. Lebedev Physical Institute, Russian Academy of Science, Leninsky Prospect 53, Moscow, Russia
(Received 5 April 1996)

The wavelengths of the $1s^2\,{}^1S_0-1snp\,{}^1P_1$ $(n=6-12)$ transitions in He-like Al XII have been measured in laser-produced and *X* pinch plasmas. The accuracy of the present measurements (0.3–0.5 mÅ) is a severalfold improvement over previous results. In addition, the resonance transitions from the $11\,{}^1P_1$ and $12\,{}^1P_1$ levels of He-like Al XII are observed. Finally, the Rydberg series is used to determine the ground-state ionization energy of Al XII, with a precision of 50 parts per million. This method gives $E_{\rm ion}=2085.98\pm0.10$ eV. These experimental results are compared with theoretical data calculated by several different methods.
[S1050-2947(96)10111-6]

PACS number(s): 32.30.Rj, 32.10.Hq, 12.20.Fv

I. INTRODUCTION

Precision measurements of transition energies provide valuable tests of the theoretical methods for calculating atomic structure. For one-electron ions, the theory is based on the Dirac equation with quantum electrodynamic (QED) effects treated by perturbation theory [1]. This approach is well understood and has been experimentally verified even for high-*Z* ions. However, no standard theoretical framework has been developed for multielectron ions, which exhibit additional effects of electron correlation and many-body QED. Theoretical and experimental studies of two-electron ions, the simplest multielectron system, have formed the basis for many of the recent advances in understanding atomic structure. In addition, heliumlike transitions have been used as reference lines to determine accurate wavelengths of transitions in other multielectron ions. The $1s^2\,{}^1S_0-1snp\,{}^1P_1$ Rydberg series naturally provide a set of closely spaced transitions useful for this purpose [2]. This provides a further need for accurate wavelengths of He-like transitions.

The theory of atomic structure of two-electron ions has been advanced considerably by the development of new computational techniques. The early calculations of Accad, Pekeris, and Schiff [3] used variational techniques that provided an accurate description of the low-lying energy levels of light He-like ions. Recently, several *ab initio* methods have been used to determine term energies for the ground and $n=2$ states for all He-like ions with $Z\leqslant100$. Boiko *et al.* used $1/Z$ expansion methods with QED corrections to calculate singlet and triplet states with angular momenta $l\leqslant2$, and $n\leqslant9$. The results are summarized in [4]. The unified method, developed by Drake [5], combined variational techniques with a relativistic $1/Z$ expansion to calculate the energies of the $n=1$ and $n=2$ states of He-like ions for all of the elements between $Z=2-100$. Plante, Johnson, and Sapirstein [6] employed an all-order, relativistic many-body perturbation technique to treat the effects of electron correlation, while retaining the QED corrections calculated in [5]. Finally, Cheng *et al.* [7] used large-scale relativistic configuration-interaction calculations, and treated QED corrections using the techniques in [8]. These calculations use different approximations and computational techniques, and some of the high-order terms remain to be calculated. Thus, experimental tests of the theory are required.

The largest effects of electron correlation and QED occur for the $1s$ orbital. Most of the experimental tests of atomic structure calculations for two-electron ions have measured $n=2-2$ transitions, for which the $1s$ contributions largely cancel. There have also been precision measurements of $n=2-1$ transitions [9–17], but these transition energies contain significant correlation and QED terms for both the $n=1$ and $n=2$ orbitals. Because the correlation and QED contributions drop rapidly with n, measurements of ground-state transitions from high-n levels directly test theoretical calculations of the ground-state ionization energy. Precision measurements of several members of the $1\,{}^1S_0-n\,{}^1P_1$ Rydberg series were measured in Refs. [14,18,19]. These measurements may be used to extract the ground-state ionization energy, as in Ref. [18]. Measurements of ionization energies for low- and medium-*Z* ions help separate the correlation energy from the QED corrections, which are more dominant in high-*Z* ions.

Wavelength measurements of the $1\,{}^1S_0-n\,{}^1P_1$ transitions from highly excited $(n\geqslant5)$ He-like states—especially for low-*Z* ions—are hindered by two effects: the low intensities of these transitions in equilibrium plasma and their broaden-

ing by plasma microfields at intermediate and high densities. In nearly steady-state plasma sources, the populations of the highly excited states drop quickly with n, making accurate measurements of these transitions difficult. The line intensities increase with density, but enhanced linewidths and background continuum emission make it difficult to identify the transitions and increase the uncertainty in the measured wavelengths. Thus, the plasma sources (vacuum sparks, tokamaks, dense laser-produced plasma, and recently electron-beam ion traps) conventionally used to investigate emission from multiply charged ions do not readily lend themselves to measurements of high-n transitions with an accuracy comparable to that of the theoretical calculations.

Different excitation mechanisms govern the line emission produced in nonstationary, recombining plasma. Here, the dependence of populations on n has a nonmonotonic character. The lines emitted from such a plasma may be narrow (because the density is low), yet intense because of the efficient pumping of the high-n levels by three-body recombination in a low-temperature, overionized plasma. Such a recombining plasma can be obtained in the process of expansion of a laser-produced plasma, or during the decay of plasma micropinches. The present work uses these two plasma sources to investigate the high-n transitions of the resonant Rydberg series of He-like aluminum ions. A focusing, spatially resolving crystal spectrometer was used to increase the measured line intensities and separate the emission of the lower density, recombining plasma from the emission from the hot, dense interaction region. These high-n transitions were used to infer the ionization energy of the Al XII ground state.

II. EXPERIMENTAL ARRANGEMENT

The experimental investigations were conducted at two experimental installations. The first set of experiments were performed at the Nd-glass laser facility at the Institute of Plasma Physics and Laser Microfusion in Warsaw, Poland [20,21]. This laser produces pulses of 6–15 J and with a 1 ns pulse duration. The laser radiation was focused on solid aluminum targets to form a spot 100–120 μm in diameter. Thus, the laser intensity on the target was about 10^{13} W/cm^2. A scheme for the experiments is shown in Fig. 1, and experimental spectra collected from the laser-produced plasma experiments are shown in Figs. 1 and 2.

The second set of experiments were conducted at the pulsed power generator BIN [22–24], operated at the P.N. Lebedev Physical Institute in Moscow, Russia. The fast-pulse storage bank consists of a Marx generator, an intermediate capacitor, a single pulse forming line and a vacuum diode. The elements were switched by gas spark gaps. The energy storage of the pulse forming line was 3.25 kJ at a charging voltage of 600 kV. The short-circuit output exceeded 270 kA. In experiments with a plasma load, the diode current reached 250 kA with a pulse of approximately 100 ns duration between the points with 10% of the maximum current.

The loads for the vacuum diode consisted of thin metal wires, spanning the 10–15 mm gap between the cathode and anode, as shown in Fig. 3. In contrast to the cases of a single wire or a liner, the hot, dense plasma is created at a fixed point, namely the point where the wires cross. In addition, due to the possibility of easy flow of material from the hot spot of the X pinch, higher specific plasma parameters can be achieved than in the case of single wires. In these experiments, 35 μm diam. aluminum wires were used.

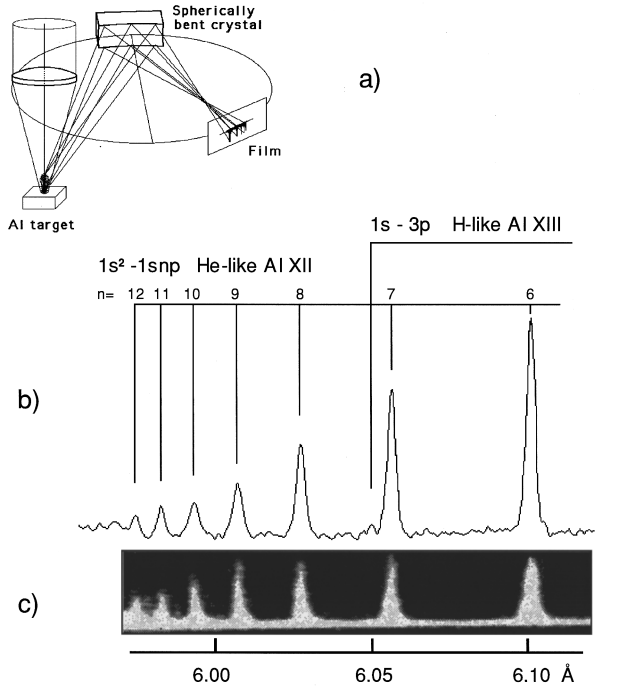

FIG. 1. (a) Schematic of the experimental arrangement for the laser-produced plasma experiments; (b) emission spectrum of aluminum transitions in the 5.95–6.13 Å region obtain by the FSSR-1D spectrograph with $2R = 186$ mm; (c) image of the film from the spectrograph.

In both cases, the plasma x-ray spectra were measured by focusing spherical crystal spectrometer with one-dimensional spatial resolution (FSSR-1D) spectrographs [25–28] containing a mica crystal bent to form a sphere of radius $2R$, where R is the radius of the Rowland circle. The general experi-

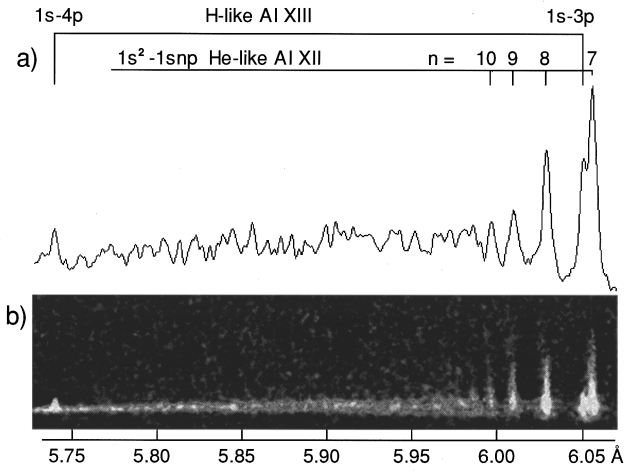

FIG. 2. (a) Spectra emitted in the aluminum laser-produced plasma experiments in the spectral region from 5.73–6.06 Å, measured with the $2R = 100$ mm FSSR-1D spectrograph; (b) an image of the film from the spectrograph.

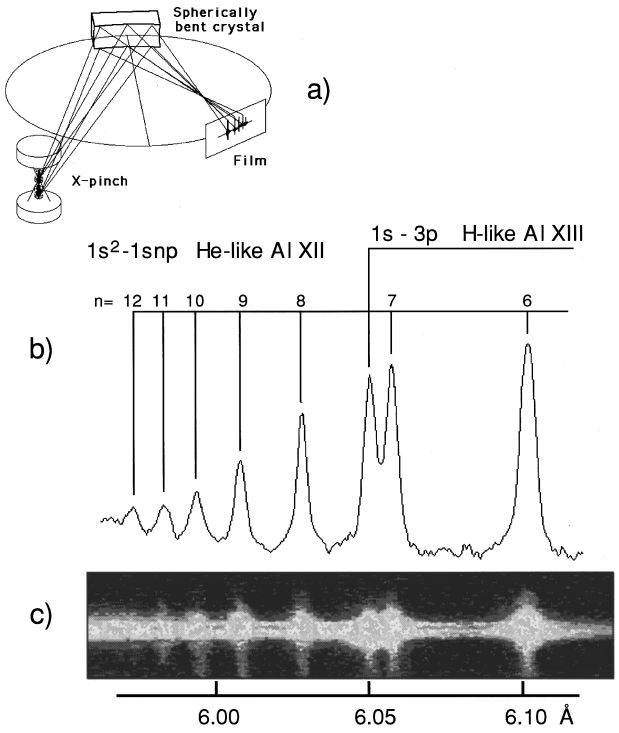

FIG. 3. (a) Schematic of the experimental arrangement for the x-pinch experiments; (b) aluminum emission spectrum measured by the FSSR-1D spectrograph with $2R=100$ mm; (c) an image of the film from the spectrograph.

mental schemes are presented in Figs. 1 and 3. The x-ray spectra were registered with one-dimensional resolution on Kodak DEF x-ray film placed on the Rowland circle. In the laser-produced plasma experiments, we used two different FSSR-1D spectrographs, one had $2R=100$ mm and the other had $2R=186$ mm. The distances between the plasma and spherically bent crystal were 173 and 255 mm, respectively. In the X-pinch experiments, a spectrograph with $2R=100$ mm placed at a distance of 137 mm from the X-pinch plasma was used. The experimental spectra are presented in Figs. 1–3. These spectra contain high members of the resonance series $1\,^1S_0-n\,^1P_1$ ($n=7-10$ for Fig. 2, and $n=6-12$ for Figs. 1 and 3), and the H-like Al XIII Lyman-β line ($1s\,^2S-3p\,^2P$). The spectrum measured from the laser-produced plasma with the $2R=100$ mm spectrograph (see Fig. 2) also contains the Lyman-γ line ($1s\,^2S-4p\,^2P$) of Al XIII.

The one-dimensional images of the plasma emission reproduced in Figs. 1–3 show that the regions of plasma creation (the target surface for the laser-produced plasma or the cross point for the X-pinch) emit wide spectral lines. The spectra emitted by these spatial regions are not suitable for accurate wavelength measurements. The use of space resolving and highly luminous FSSR-1D spectrographs allowed us to observe the spectra radiated from the low-density plasma regions, where the spectral linewidths were small enough (about 3 mÅ) that wavelength measurements with a relative accuracy $\Delta\lambda/\lambda\approx(5-8)\times10^{-5}$ were possible.

We conclude this section with a discussion of the potential sources of line shifts that could influence the precision of the measurements. These include shifts induced by high plasma density, high-n satellites, or plasma motion. In the low-density regions used for the wavelength measurements, the plasma density shifts are very small, much smaller than the linewidths. These regions also have low temperatures and the satellite lines are not effectively excited. While ground-state transitions are easily produced in an overionized plasma by recombination processes at any temperature, the multiply excited satellite levels are produced by processes that have large energy thresholds and are suppressed at low temperatures. At the distances from the point of plasma creation where these spectra were emitted, no satellite lines were observed. The shifts induced by plasma motion were limited because the viewing angle of the spectrometer was almost perpendicular to the main direction of motion. In addition, the spectra were calibrated by H-like reference lines emitted from the same plasma region as the transitions we investigated. Any residual doppler shifts would largely cancel. Thus, the linewidths are the main limitation on the precision of these measurements.

III. RESULTS AND DISCUSSION

The wavelength measurements of the $1\,^1S_0-n\,^1P_1$ Al XII lines were carried out in two steps. First, the wavelengths of the transitions for $n=7-10$ were measured using the spectrum from the laser-produced plasma shown in Fig. 2. In this procedure the Lyman-β and Lyman-γ Al XIII lines were used as reference lines and the dispersion function of FSSR-ID spectrograph was taken in quasi-Johann form:

$$n\lambda=2d(1+x/a_1)\cos(x/2R), \tag{1}$$

where $2d$ is the interplanar crystal spacing, n the order of reflection, x the position on the film, and the multiplier $(1+x/a_1)$ corrects for the deflection of the film from the Rowland circle, with parameter a_1 determined from the wavelengths of the reference lines. The reference line wavelengths were taken from the calculations in [4]. The uncertainty of these calculated wavelengths is about ±0.007 mÅ, much smaller than the experimental precision of $\pm(0.3-0.5)$ mÅ. The experimental accuracy at this step was limited mainly by the widths of the observed spectral lines, because the Lyman-β and Lyman-γ Al XIII reference lines were emitted mainly from relatively dense plasma regions. The measured wavelength values are presented in column e of Table I.

In the second step, spectra obtained by the $2R=186$ mm spectrograph in laser-produced plasma (Fig. 1) and by the $2R=100$ mm spectrograph in X-pinch (Fig. 3) were analyzed. These spectra were calibrated using the wavelengths of the $1\,^1S_0-7\,^1P_1$, $1\,^1S_0-8\,^1P_1$, $1\,^1S_0-10\,^1P_1$, as reference values; the wavelengths of $1\,^1S_0-8\,^1P_1$, $1\,^1S_0-9\,^1P_1$, $1\,^1S_0-11\,^1P_1$, and $1\,^1S_0-12\,^1P_1$ spectral lines were measured. The dispersion function was as in Eq. (1), however the use of three reference lines allowed the quadratic term in the film deflection correction $(1+x/a_1+x^2/a_2)$ to be taken into account. This additional correction had only a minor effect. The accuracies of these measured wavelengths were limited by the accuracies of the reference wavelengths, except for the values for the $1\,^1S_0-11\,^1P_1$ and $1\,^1S_0-12\,^1P_1$ transitions, which were limited by their linewidths. The results of these measurements are presented in columns f and g of Table I for laser-produced plasma and X-pinch plasma ex-

TABLE I. Theoretical and experimental wavelengths of resonance transitions of Al XII and Al XIII ions.

Ion	Transition	Theory wavelengths (Å)				Experimental wavelengths (Å)		
		λ^a	λ^b	λ^c	λ^d	λ^e	λ^f	λ^g
Al XIII	$4p\,^2P_{3/2,1/2}-1s\,^2S_{1/2}$		5.739 27[h]			5.739 27[i]		
Al XII	$1s12p\,^1P_1-1s^2\,^1S_0$	5.982 72			5.982 71		5.982 78(50)	5.982 71(55)
Al XII	$1s11p\,^1P_1-1s^2\,^1S_0$	5.990 19			5.990 18		5.989 81(50)	5.990 23(55)
Al XII	$1s10p\,^1P_1-1s^2\,^1S_0$	6.000 03		6.000 04	6.000 03	6.000 35(40)	6.000 35[i]	6.000 35[i]
Al XII	$1s9p\,^1P_1-1s^2\,^1S_0$	6.013 40	6.013 40	6.013 40	6.013 40	6.013 14(40)	6.013 23(40)	6.013 40(40)
Al XII	$1s8p\,^1P_1-1s^2\,^1S_0$	6.032 17	6.032 19	6.032 19	6.032 18	6.032 55(40)	6.032 55[i]	6.032 55[i]
Al XIII	$3p\,^2P_{3/2,1/2}-1s\,^2S_{1/2}$		6.052 91[h]			6.052 91[i]		6.052 82(40)
Al XII	$1s7p\,^1P_1-1s^2\,^1S_0$	6.059 76	6.059 76	6.059 79	6.059 78	6.060 07(30)	6.060 07[i]	6.060 07[i]
Al XII	$1s6p\,^1P_1-1s^2\,^1S_0$	6.102 76	6.102 76	6.102 82	6.102 79		6.102 81(40)	6.102 79(40)

[a]Present calculations.
[b]Calculations from Ref. [2].
[c]Calculations from Ref. [14].
[d]Quantum-defect approximation used to extend data from Ref. [2].
[e]Experiment with laser-produced plasma ($2R=100$ mm spectrograph).
[f]Experiment with laser-produced plasma ($2R=186$ mm spectrograph).
[g]Experiment with *X*-pinch plasma.
[h]Statistically weighted for doublet lines.
[i]Used as reference lines.

periments, respectively. There is very good agreement between the different experimental measurements.

Theoretical wavelength calculations obtained by several different methods for the $1\,^1S_0-n\,^1P_1$ ($n=6-12$) transitions are presented in Table I. The largest inaccuracies in these calculations arise from the effects of electron correlation and QED. Since these effects are quite small for the $1snp$ states with $n\geq 6$, the theoretical uncertainty is dominated by the ground-state energy calculation. The wavelength values in column a were derived from Drake's [5] ground-state ionization energy and excited-state term energies obtained from the relativistic, multiconfiguration parametric potential atomic structure code RELAC [29]. In this code the radial wave functions are calculated assuming the electrons move in a central potential, which is an analytic function of screening parameters. These parameters are determined by minimizing the first-order relativistic energy of the excited configurations. The self-energy is scaled from results of Mohr [30] and Erickson [31] using an effective charge for each orbital that would reproduce the average radius in a hydrogenic calculation. The Breit interaction is included in the long wavelength limit.

Column b in Table I presents calculations from Ref. [4] for the transitions with $6\leq n\leq 9$. These were obtained from a $1/Z$ expansion method, including relativistic and QED effects. Results from Ref. [32] for $6\leq n\leq 10$ are given in column c. These wavelengths were obtained from a series formula [33] derived from Drake's calculations for the $n=1,2$ levels [5] and term energies from Ermolaev and Jones [34] for $n=3-5$. Finally, the calculations from column b were extended to higher n by fitting the data from Ref. [4] to obtain the n dependence of the quantum defect. The wavelengths obtained by this procedure are given in column d.

As shown in Table I, there is a very good agreement between the different sets of theoretical wavelengths. This is because the present work and the values of Martin both used Drake's ground-state ionization energy (16 824 529 cm^{-1}), which is almost identical to the value (16 824 530 cm^{-1}) obtained in Ref. [4].

The Rydberg series of $1\,^1S_0-n\,^1P_1$ transitions in He-like Al can be used to derive the ground-state ionization energy, using a procedure similar to [18]. Following Martin [33], the measured wavelengths for the Rydberg series were fit to an expression:

$$\frac{1}{\lambda_n}=E_{\rm ion}-\frac{R_Z(Z-1)^2}{(n-a-b/n^2)^2}, \tag{2}$$

where $E_{\rm ion}$ is the ground-state ionization energy, R_Z is the Rydberg constant for Al XII, and a and b are parameters in a quantum defect fit to the measured wavelengths. Following Ref. [5], the value $R_Z=109\,735.0840\ cm^{-1}$ was adopted. For the transitions which were independently measured, the three sets of wavelength measurements listed in Table I were combined. Because the $n\geq 6$ transitions are insensitive to the value of b in Eq. (2), the wavelengths measured in the present experiments were supplemented with the value $\lambda=7.7573$ for the $1\,^1S_0-2\,^1P_1$ transition [35], to constrain the value of b obtained by the fitting procedure to physically reasonable values. The ionization energy obtained by this method was unaffected by variations of this $n=2-1$ wavelength as large as tens of milliangstroms.

The ionization energy obtained from fitting the experimental wavelengths to Eq. (2) is compared to several theoretical calculations in Table II. Also shown are the experimental transition energies obtained by combining the three experimental measurements, and the transitions energies given by Eq. (2). The deduced ionization energy, 16 824 520 $\pm 800\ cm^{-1}$ (2085.98$\pm$0.100 eV) agrees well with the theoretical values. The experimental uncertainty is dominated by the uncertainty in the wavelength calibration. This experimental uncertainty is roughly 30% of the QED correction

TABLE II. Ground-state ionization energy and excitation energies of Al XII $1snp\ ^1P_1$ levels.

Level[a]	Experiment (1000 cm^{-1}) E_{expt}[b]	Theory (1000 cm^{-1}) E_{theor}[c]	E_{fit}[d]	E_{ion}[e]	E_{ion}[f]	E_{ion}[g]	E_{ion}[h]
$1s6p\ ^1P_1$	16 385.9 (0.5)	16 386.0	16 385.6				
$1s7p\ ^1P_1$	16 501.5 (0.6)	16 502.3	16 502.0				
$1s8p\ ^1P_1$	16 576.7 (0.8)	16 577.8	16 577.6				
$1s9p\ ^1P_1$	16 629.9 (0.4)	16 629.5	16 629.4				
$1s10p\ ^1P_1$	16 665.7 (0.8)	16 666.6	16 666.5				
$1s11p\ ^1P_1$	16 694.4 (0.7)	16 694.0	16 693.9				
$1s12p\ ^1P_1$	16 714.7 (0.7)	16 714.8	16 714.8				
E_{ion}			16 824.52 (0.80)	16 824.530	16 824.529	16 824.542	16 824.584

[a]Upper state of ground-state excitation, E_{ion} is ground-state ionization energy.
[b]Experimental energies obtained by combining measurements in Table I: Value for E_{ion} is extracted as described in text. The numbers in parentheses are experimental uncertainties.
[c]Theoretical energies from present calculations.
[d]Energies obtained by fitting experimental energies with Eq. (2). The number in parentheses after E_{ion} value is the experimental uncertainty.
[e]Ionization energy from Ref. [4].
[f]Ionization energy from Ref. [5].
[g]Ionization energy from Ref. [6].
[h]Ionization energy from Ref. [37].

[36] and 10% of the electron correlation contribution to the ionization energy. Thus, the present measurement provides a direct test of calculations of the electron correlation and many-body QED contributions to the ground-state ionization energy of Al XII. However, this measurement cannot distinguish between the modern theories of two-electron ions.

IV. CONCLUSIONS

High-n members of the $1\ ^1S_0-n\ ^1P_1$ Al XII transitions ($n=6-12$) were measured with an accuracy $\Delta\lambda/\lambda\approx 5-8\times10^{-5}$ Å and used to deduce the ground-state ionization energy with an uncertainty of 50 parts per million. The deduced ionization energy, $16\,824\,520\pm800$ cm^{-1}, agrees well with recent theoretical calculations. The transition wavelengths were measured with an accuracy three to four times smaller than previous measurements for $n\leqslant10$. In addition, these measurements include high-precision measurements of the wavelengths for the $1\ ^1S_0-n\ ^1P_1$ transitions for $n=11$, 12. These results test recent theories of electron correlation and quantum electrodynamics in two-electron systems.

ACKNOWLEDGMENTS

The authors thank K. T. Cheng for helpful discussions and for providing unpublished results for this work. This work was supported in part by the Russian Fund for Fundamental Research Project No. 93-02-15410 and the International Science Foundation Grant No. N MBJ000. The work at Lawrence Livermore National Laboratory was performed under the auspices of the U.S. Department of Energy under Contract No. W-7405-Eng-48.

[1] P. J. Mohr, Phys. Rev. A **46**, 4421 (1992).
[2] P. Beiersdorfer, A. Osterheld, S. R. Elliott, M. H. Chen, D. Knapp, and K. Reed, Phys. Rev. A **52**, 2693 (1995).
[3] Y. Accad, C. L. Pekeris, and B. Schiff, Phys. Rev. A **4**, 516 (1971).
[4] V. A. Boiko, V. G. Palchikov, I. Yu. Skobelev, and A. Ya. Faenov, *Spectroscopic Constants of Atoms and Ions (Spectra of Atoms with One and Two Electrons)* (Izdatel'stvo Standart, Moscow, 1988) (in Russian).
[5] G. W. F. Drake, Can. J. Phys. **66**, 586 (1988); Zon-Chao Yan and G. W. F. Drake, Phys. Rev. Lett. **74**, 4791 (1995).
[6] D. R. Plante, W. R. Johnson, and J. Sapirstein, Phys. Rev. A **49**, 3519 (1994).
[7] K. T. Cheng, M. H. Chen, W. R. Johnson, and J. Sapirstein, Phys. Rev. A **50**, 247 (1994).
[8] K. T. Cheng, W. R. Johnson, and J. Sapirstein, Phys. Rev. A **47**, 1817 (1993); Phys. Rev. Lett. **66**, 2960 (1991).
[9] L. Schleinkofer, F. Bell, H.-D. Betz, G. Trollmann, and J. Rothermel, Phys. Scr. **25**, 917 (1982).
[10] J. P. Briand, J. P. Mosse, P. Indelicato, P. Chevallier, D. Girard-Vernhet, and A. Chetioui, Phys. Rev. A **28**, 1413 (1983).
[11] P. Indelicato, J. P. Briand, M. Tavernier, and D. Liesen, Z. Phys. D **2**, 249 (1986).
[12] R. D. Deslattes, H. F. Beyer, and F. Folkmann, J. Phys. B **17**, L687 (1984).
[13] J. P. Briand, M. Tavernier, R. Marruss, and J. P. Desclaux, Phys. Rev. A **29**, 3143 (1984).
[14] P. Beiersdorfer, M. Bitter, S. von Goeler, and K. W. Hill, Phys. Rev. A **40**, 150 (1989).

[15] J. P. Briand, P. Indelicato, A. Siminovici, V. San Vicente, D. Liesen, and D. Dietrich, Europhys. Lett. **9**, 225 (1989).
[16] J. P. Briand, P. Chevallier, P. Indelicato, K. P. Ziock, and D. D. Dietrich, Phys. Rev. Lett. **65**, 2761 (1990).
[17] S. MacLaren, P. Beiersdorfer, D. A. Vogel, D. Knapp, R. E. Marrs, K. Wong, and R. Zasadzinski, Phys. Rev. A **45**, 329 (1992).
[18] J. F. Seeley and U. Feldman, Phys. Rev. Lett. **54**, 1016 (1985).
[19] P. Indelicato, O. Gorceix, M. Tavernier, J. P. Briand, J. P. Desclaux, R. Marrus, and M. Prior, Z. Phys. D **2**, 149 (1986).
[20] V. M. Dyakin, T. A. Pikuz, I. Yu. Skobelev, A. Ya. Faenov, J. Wolowski, L. Karpinski, A. Kasperczyk, T. Pisarczyk, Quantum Electron. **21**, 1186 (1994).
[21] V. M. Dyakin, A. Ya. Faenov, A. I. Magunov, J. Makowski, P. Parys, T. A. Pikuz, T. Pisarczyk, I. Yu. Skobelev, J. Wolowski, and E. Woryna, Phys. Scr. **52**, 201 (1995).
[22] S. A. Pikuz, B. A. Bryunetkin, G. V. Ivanenkov, A. R. Mingaleev, V. M. Romanova, I. Yu. Skobelev, A. Ya. Faenov, S. Ya. Khalhalin, and T. A. Shelkovenko, Quantum Electron. **23**, 201 (1993).
[23] S. A. Pikuz, B. A. Bryunetkin, G. V. Ivanenkov, A. R. Mingaleev, V. M. Romanova, I. Yu. Skobelev, A. Ya. Faenov, S. Ya. Khakhalin, and T. A. Shelkovenko, J. Quantum Spectrosc. Radiat. Transfer **51**, 291 (1994).
[24] A. Ya. Faenov, S. A. Pikuz, A. I. Erko, B. A. Bryunetkin, V. M. Dyakin, G. V. Ivanenkov, A. R. Mingaleev, T. A. Pikuz, V. M. Romanova, and T. A. Shelkovenko, Phys. Scr. **50**, 333 (1994).
[25] B. A. Bryunetkin, S. A. Pikuz, I. Yu. Skobelev, and A. Ya. Faenov, Laser Part. Beams **10**, 849 (1992).
[26] A. Ya. Faenov, V. A. Agafonov, B. A. Bryunetkin, A. I. Erko, G. V. Ivanenkov, A. R. Mingaleev, S. A. Pikuz, V. M. Romanova, T. A. Shelkovenko, and I. Yu. Skobelev, in *Applications of Laser Plasma Radiation*, edited by Martin C. Richardson (SPIE, Bellingham, 1994), Vol. 2015, p. 64.
[27] S. A. Pikuz, V. M. Romanova, T. A. Shelkovenko, T. A. Pikuz, A. Ya. Faenov, E. Foerster, I. Vol'f, and O. Verhan, Quantum Electron. **22**, 21 (1995).
[28] J. Nilsen, P. Beiersdorfer, S. R. Elliott, T. W. Phillips, B. A. Bryunetkin, V. M. Dyakin, T. A. Pikuz, A. Ya. Faenov, S. A. Pikuz, P. A. Loboda, V. A. Lykov, and V. Yu. Politov, Phys. Rev. A **50**, 2143 (1994).
[29] M. Klapisch, Comput. Phys. Commun. **2**, 239 (1971); M. Klapisch, J. L. Schwob, B. S. Fraenkel, and J. Oreg, J. Opt. Soc. Am. B **61**, 148 (1977).
[30] P. J. Mohr, Atom. Data Nucl. Data Tables **29**, 453 (1983).
[31] G. W. Erickson, J. Phys. Chem. Ref. Data **6**, 831 (1977).
[32] V. Kaufman and W. C. Martin, J. Phys. Chem. Ref. Data **20**, 777 (1991).
[33] W. C. Martin, Phys. Scr. **24**, 725 (1981).
[34] A. M. Ermolaev and M. Jones, J. Phys. B **7**, 199 (1974), and unpublished supplement.
[35] H. Flembeg, Ark. Mat. Astron. Fys. **28**, 1 (1942), adjusted for conversion from x units to Å in W. C. Martin, Phys. Scr. **24**, 725 (1981).
[36] P. Indelicato, Phys. Rev. A **51**, 1132 (1995).
[37] K. T. Cheng (private communication), using techniques of K. T. Cheng, M. H. Chen, W. R. Johnson, and J. Sapirstein, Ref. [7].